

# Nuclear Fusion Enhancement by Heavy Nuclear Catalysts

Christopher Grayson<sup>1</sup>, Johann Rafelski<sup>2</sup>

<sup>1</sup>Wigner Research Centre for Physics, 1121 Budapest, Hungary

<sup>2</sup>Department of Physics, The University of Arizona, Tucson, Arizona 85721, USA

**Abstract.** We seek to understand the effect of high electron density in the proximity of a heavy nucleus on the fusion reaction rates in a hot plasma phase. We investigate quantitatively the catalytic effect of gold ( $Z = 79$ ) ions embedded in an electron plasma created due to plasmonic focusing of high-intensity short laser pulses. Using self-consistent strong plasma screening, we find highly significant changes in the internuclear potential of light elements present nearby. For gold, we see a 14 keV change in the internuclear potential near the nuclear surface, independent of the long-distance thermal Debye-Hückel screening. The dense polarization cloud of electrons around the gold catalyst leads to a  $\sim 1.5$  enhancement of proton-boron ( ${}^1\text{B}$ ) fusion above  $T = 100$  keV.

## 1 Introduction

This article expands on the work in [1] relating it to fusion enhancement in gold nanoparticle-doped fusion targets. In the earlier work [1], the effect of self-consistent screening of light nuclei during Big Bang nucleosynthesis (BBN) was found to lead to a small correction for thermonuclear reactions but to have a very strong dependence on nuclear charge  $Ze$ . This article investigates self-consistent strong screening of “heavy nuclear catalyst” or high  $Z$ -ionic impurities in a plasma.

Heavy nuclear catalysts, such as gold ( $Z = 79$ ), generate a dense local screening cloud of electrons within a hot plasma. The Coulomb barrier is significantly reduced within the electron cloud, and lighter nuclei can more easily participate in thermonuclear reactions. Dispersed gold ions are often present in plasma generated in laser-fusion experiments using gold film [2,3], in the hohlraum used in inertial confinement fusion experiments [4,5], and introduced by plasmonic gold nanoparticles [6,7,8,9,10,11,12,13,14]. In these plasmonic nanoparticle experiments, a huge number of conducting electrons oscillate with the electromagnetic field of an ultrafast pulse laser in a localized surface plasmonic resonance (LSPR). The screening enhancement of fusion reactions could occur locally within the cloud of conducting electrons around these nanorods. The electron cloud oscillation in an LSPR is a coherent quantum process. We explore this concept semi-classically by analogy using a high-temperature electron-ion plasma around an ionized gold nucleus.

Self-consistent strong screening refers to solving the Poisson equation, including the induced charge density, without any approximation in its dependence on the electric potential  $\phi$ . In this case, the charge density is a nonlinear function of the solution potential  $\phi$ . Electrons surround an ion’s charge  $Ze$  (elementary charge  $e >$

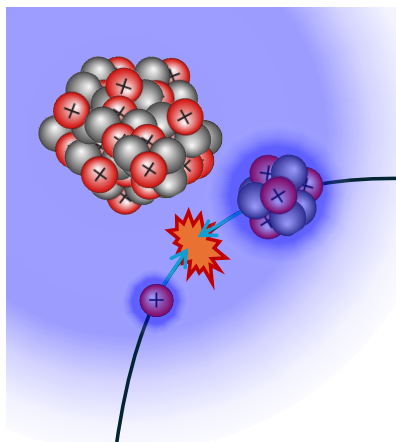


**Fig. 1.** Depiction of heavy nuclei catalyzing fusion reactions. Two particles (proton and boron) collide in the presence of a large screening cloud of electrons generated by a stationary heavy nucleus such as Au ( $Z = 79$ ).

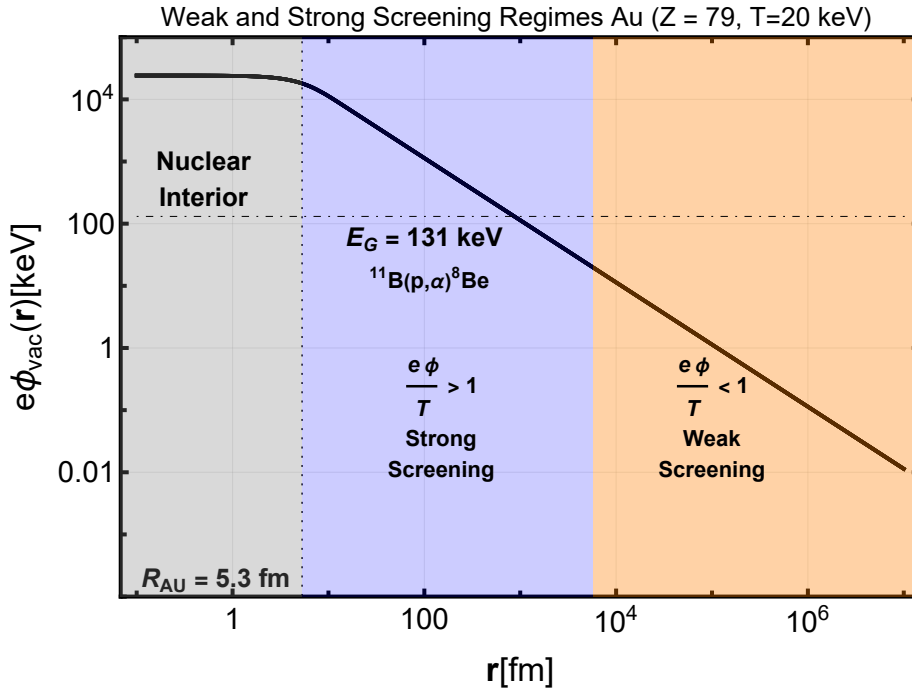


**Fig. 2.** We show the ratio of the electromagnetic potential energy to the thermal energy for the vacuum potential of gold nuclei. The portion of the potential with strong screening corrections is shown in purple, and the weak screening region is shown in orange. The Gamow energy Eq. (3) for a proton boron reaction probes the strong screening regime

0), which reduces the electromagnetic influence of other nuclear charges at large distances. In the context of nuclear reactions, this reduction in electrostatic repulsion reduces the Coulomb barrier and facilitates an increased penetration probability. This implies that electromagnetic screening increases thermonuclear reaction rates [15]. Heavy nuclear catalysts are high  $Z$  nuclei, which provide a large screening cloud with which lighter nuclei can enter and more easily undergo thermonuclear reactions. This process is depicted in Fig. 1 where two light nuclei collide in the screening cloud of a third stationary heavy nucleus ( $m_{\text{Au}} \gg T$ ), which acts as a catalyst for the reaction.

Often plasma studies assume the “weak-field” limit where the electromagnetic potential energy  $q\phi(r)$  is small compared to the thermal energy  $T$

$$\frac{q\phi(r)}{T} \ll 1, \quad (1)$$

where we set Boltzmann’s constant  $k_B = 1$ . Plasmas satisfying this condition are weakly coupled, and plasma effects lead to linear corrections to the potential, as in Debye-Hückel theory [16].

Even if a plasma is weakly coupled, nonlinear corrections to the potential may be relevant in thermonuclear reactions. This is because the Gamow energy  $E_G$ , the energy at most reactions occur, is higher than thermal energy [17] and probes the short-distance electromagnetic potential. The inter-nuclear distance corresponding to Gamow energy is typically on the order of femtometers, such that the weak screening condition is not satisfied for the short-range potential relevant to the Coulomb barrier

$$\frac{Ze\phi(r_{E_G})}{T} > 1, \quad (2)$$

where  $r_{E_G}$  is the classical turning point at the Gamow energy.

$$E_G = \left( \frac{(\pi T Z_1 Z_2 \alpha)^2 \mu_r}{2} \right)^{1/3}. \quad (3)$$

The reduced mass of the colliding light nuclei is  $\mu_r$ , and  $Z_1$  and  $Z_2$  are the respective charges of the nuclei. As depicted in Fig. 2, the condition Eq. (2) implies that although a plasma may be treated as weakly coupled at large distances, locally, the short-range potential can have nonlinear corrections simply because the electrostatic energy close to a nucleus can be much higher than the thermal energy.

The self-consistent strong polarization potential is described by the Poisson-Boltzmann equation [18,19,20,21,22,23,24,1]. We solve the Poisson-Boltzmann equation directly by implementing a finite-sized source charge density and using Fermi-Dirac statistics. This description of screening reproduces the Thomas-Fermi model in the zero temperature limit and Debye-Hückel screening in the high temperature  $\phi/T \ll 1$  limit. This allows us to simultaneously describe bound electrons and outer electrons, which join the thermal screening cloud in the

plasma at various temperatures. The Poisson Boltzmann equation is also relevant to describe the sheath potential in Target Normal Sheath Acceleration (TNSA) [25,26].

Self-consistent strong screening differs from other ‘strong screening’ models [15,27,28,29,30,31,32,33] developed for white dwarfs which are applicable for plasmas where the Coulomb energy is much larger than the thermal energy. Models studying strong screening are typically interested in plasmas with a Coulomb coupling parameter

$$\Gamma_e = \frac{Z_1 Z_2 \alpha \hbar c}{T a_e}, \quad \text{with} \quad a_e = \left( \frac{3}{4\pi n_e} \right)^{1/3}, \quad (4)$$

which is  $1 \leq \Gamma_e \leq 200$ . In this work, we study ‘intermediate screening,’ which we call self-consistent strong screening since it captures both the strong and weak field regimes.

Section 2 reviews the theoretical background of self-consistent strong screening. Section 3 presents numerical solutions to the Poisson-Boltzmann equation for heavy Au particles in a laser plasma. Section 4 estimated the reaction rate enhancement for proton boron fusion. Section 5 reviews our results and discusses their implications for fusion.

## 2 Self-consistent strong screening of heavy nuclear catalysts

We find the total potential  $\phi(r) = \phi_{\text{ext}}(r) + \phi_{\text{ind}}(r)$  in plasma by solving the Poisson equation with the induced polarization charge density  $\rho_{\text{ind}}(r)$  and the external charge density of the light nuclei  $\rho_{\text{ext}}(r)$

$$-\nabla^2 \phi(r) = \rho_{\text{tot}}(r)/\varepsilon_0 = [\rho_{\text{ext}}(r) + \rho_{\text{ind}}(r)]/\varepsilon_0, \quad (5)$$

where  $\varepsilon_0$  is the vacuum permittivity. The equilibrium-induced charge density is the difference between the charge density of electrons and protons

$$\rho_{\text{ind}}(r) = en_p(r) - en_-(r) \approx -en_-(r), \quad (6)$$

where  $n_-(r)$  represents the number density of electrons and  $n_p(r)$  of protons. We study the electron plasma at keV energies, which forms from the laser interaction with matter for intensities of  $10^{17} - 10^{20}$  W/cm<sup>2</sup> on timescales of 20 fs. On this time scale, we assume electrons in the plasma are approximately at thermal equilibrium and ions have not yet reacted since they are not mobile enough to participate in screening due to their much larger mass. Including plasma dynamics in the self-consistent strong screening is the subject of future work.

We introduce the unit-less potential

$$\Phi(r) \equiv \frac{e\phi(r)}{T}, \quad (7)$$

which compares the Coulomb energy  $e\phi$  to the plasma temperature  $T$ . Similarly we introduce the re-scaled external charge distribution  $P_{\text{ext}}$

$$P_{\text{ext}}(r) \equiv e \frac{\rho_{\text{ext}}(r)}{\varepsilon_0 T} = \frac{4\pi Z \alpha \hbar c}{\pi^{3/2} R^3 T} e^{-\frac{r^2}{R^2}}, \quad (8)$$

we chose to model the charge distribution of a nucleus as a Gaussian to make self-consistent screening soluble. Here  $R$  is the root-mean-squared charge radius

$$R = \sqrt{\frac{2}{3}} R_{\text{Au}}. \quad (9)$$

For the radius of an Au (gold) atom, we use the charge radius  $R_{\text{Au}} = 5.3$  fm [34]. We rewrite the Poisson equation Eq. (5) using the effective screening mass defined in [1]

$$\frac{m_s^2(\Phi)}{(\hbar c)^2} \equiv -\frac{e\rho_{\text{ind}}(r)/(\varepsilon_0 T)}{\Phi(r)}. \quad (10)$$

The screening mass  $m_s^2$  is related to the usual Debye screening mass in the weak screening limit

$$\frac{m_s^2(\Phi \ll 1)}{(\hbar c)^2} \approx \frac{m_D^2}{(\hbar c)^2} = \frac{1}{\lambda_D^2} = \frac{4\pi\alpha\hbar c}{T} n_{\text{eq}}. \quad (11)$$

but exhibits additional nonlinear behavior due to its dependence on the potential. Using this screening mass Eq. (5) takes a form which is analogous to Debye-Hückel theory

$$-\nabla^2 \Phi(r) + \frac{m_s^2(\Phi)}{(\hbar c)^2} \Phi(r) = P_{\text{ext}}(r), \quad (12)$$

Which is then solved numerically for  $\Phi(r)$ . We describe the screening as using the relativistic Fermi-Dirac distribution [1]

$$f_F^\pm(x, p) = \frac{1}{\exp[u_\mu(p^\mu + qA^\mu(x))] / T + 1}. \quad (13)$$

where  $q = \pm e$  is the charge of the fermions,  $u_\mu = (1, 0, 0, 0)$  is the global velocity of the plasma, and  $A^\mu$  is the 4-potential in the plasma. The screening mass for the Fermi-Dirac distribution for electrons is

$$m_{s, \text{FD}}^2(\Phi) = \frac{4\pi\alpha}{T\Phi(r)} \int \frac{d^3\mathbf{p}}{(2\pi)^3} \frac{1}{\exp(p_0/T - \Phi(r)) + 1}, \quad (14)$$

where  $p_0 = \sqrt{|\mathbf{p}|^2 + m^2}$ . In the limit,  $T \rightarrow 0$  Eq. (14) returns the usual relativistic Thomas-Fermi model. For convenience, we use the electron-positron plasma Debye mass from [1] removing the factor of 2 accounting for the two species, which matches Eq. (14) for  $\phi/T > 1$ .

$$m_{s, \text{FD}}^2(\Phi) \approx \frac{4\pi\alpha}{T\Phi(r)} \int \frac{d^3\mathbf{p}}{(2\pi)^3} \frac{\sinh[\Phi(r)]}{\cosh(p_0/T) + \cosh[\Phi(r)]}, \quad (15)$$

this ensures the plasma is neutral at large distances, which is not true in Eq. (14) where only electrons are considered. In a more exact model, we would use a chemical potential to specify the distribution of electrons and protons such that the plasma is neutral. However, since the Debye mass is calculated in the static limit, it is not sensitive to the mass difference of electrons and ions, only the density of charges, which would, in principle, be the same. It would be more important to fix the density to those found in electron plasmas formed during laser interactions with matter, but this is the subject of future work.

### 3 Solving the strong field Poisson equation self consistently

The numerical solution method to Eq. (12) is described in [1]. To summarize, we start the integration of Eq. (12) at large values of  $r$  where the weak field condition Eq. (1) applies since there once can find an analytic Debye type solution, up to an overall normalization due to the additional screening that will occur at short ranges. One can integrate inwards with any standard solver to small values of  $r$  varying a shooting parameter  $Q_{\text{eff}}$  until the solution converges sufficiently close to  $r = 0$ .

We are interested in the potential due to screening charges  $\phi_{\text{ind}}$  where

$$\phi_{\text{ind}}(r) \equiv \phi(r) - \phi_{\text{vac}}(r), \quad (16)$$

with  $\phi$  being the total potential in the plasma and  $\phi_{\text{vac}}$  the potential in vacuum. The induced polarization potential  $\phi_{\text{ind}}(0)$  is the potential due to the screening electron cloud and is responsible for the reduction of electrostatic potential energy between charges. The potential difference  $\phi_{\text{ind}}(0)$  is proportional to the change in the internuclear potential at the origin, often denoted as  $H(0)$ , which is related to screening enhancement of reaction rates  $\mathcal{F}_{\text{sc}}$  [15]

$$\mathcal{F}_{\text{sc}} \sim \exp\left(\frac{H(0)}{T}\right) \sim \exp\left(\frac{e\phi_{\text{ind}}(0)}{T}\right). \quad (17)$$

The quantity  $\phi_{\text{ind}}(r)$  is plotted for a gold ion in Fig. 3. Self-consistent strong screening predicts a larger induced polarization potential than weak screening due to its nonlinear dependence on the potential, which is exponential in the Boltzmann limit [1]. This effect is more pronounced near the origin where  $e\phi/T$  is large. The dashed lines show the weak polarization potential, which is nearly constant up to distances  $\lambda_D$  and equal to its value at the origin

$$e\phi_{\text{ind}}(0) = Z\alpha m_D. \quad (18)$$

In Fig. 3, the overlapping inner blue curves show the potential due to electrons bound to gold, while the outer red curve shows the potential due to the thermal screening cloud. This is because Eq. (12) reduces to Thomas-Fermi Theory in the zero temperature limit and returns Debye-Hückel screening in the large distance limit  $e\phi(\infty)/T \ll 1$ . We can interpret the transition from the inner set of blue curves to the parallel larger distance red curves as outer electrons joining the Debye-Hückel type thermal screening cloud at increasing temperatures.

In Fig. 3, we see that the self-consistent strong screening contribution to the potential near the origin is additive to the weak screening contribution Eq. (18). By subtracting the weak screening contributions, shown as dashed lines, from the full solution at each temperature, we find the strong screening contribution for gold ( $Z=79$ ) independent of temperature around 14.2 keV. This should be close to the electric potential shift due to the electron cloud around a gold atom at zero temperature. Using the numerical fit for the shift in the potential from Hartree-Fock wavefunctions [35], and estimating the Thomas-Fermi constant  $a_{\text{TF}}$  from the tabulated values in [35] for  $Z = 79$ ,  $a \approx 1.598$ , we find

$$e\phi_{\text{HF}}(0) = \alpha^2 Z^{4/3} a_{\text{TF}} m_e = 14.7 \text{ keV}. \quad (19)$$

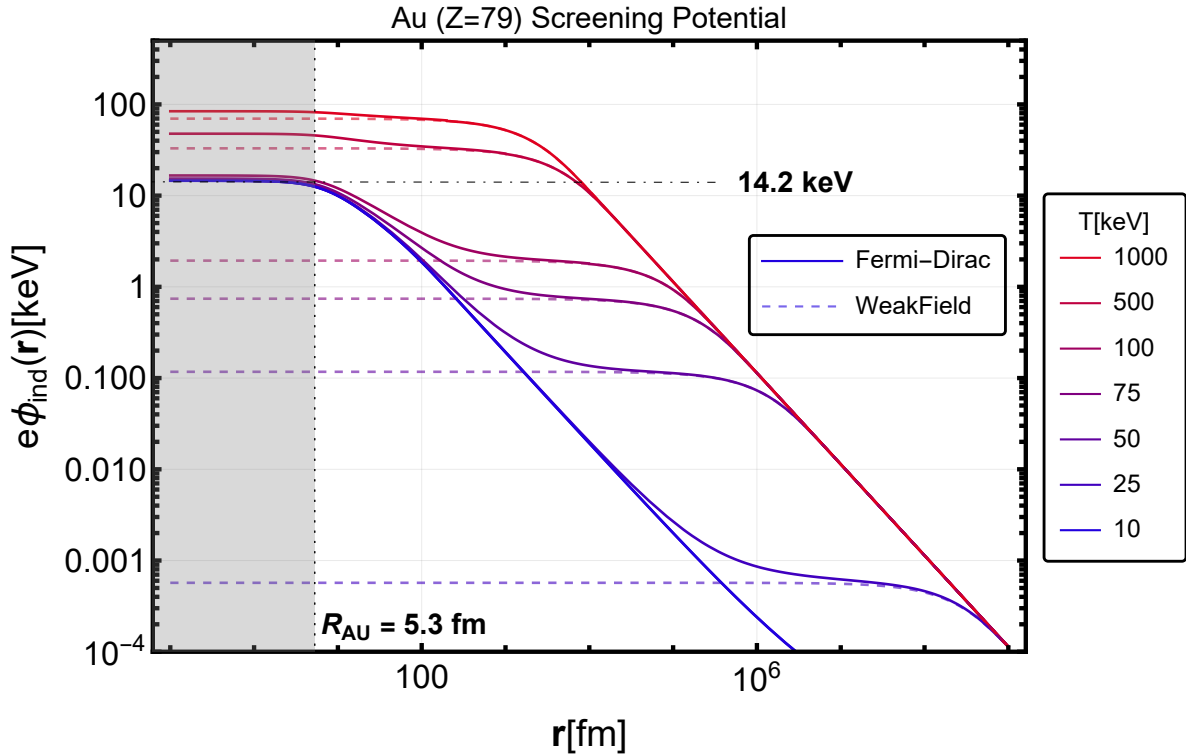


**Fig. 3.** The potential  $e\phi_{\text{ind}}$  due to the induced screening charge density for Fermi-Dirac self-consistent strong screening Eq. (13) at various temperatures is shown as solid lines ranging from blue to red. The weak polarization potential is shown as dashed lines ranging from blue to red. Overall screening decreases with temperature  $T$ , but the difference between weak and strong becomes larger for small  $T$ . The gray area shows the nuclear interior at a radius of  $R_{\text{Au}} = 5.3 \text{ fm}$ , where the nuclear potential would take over.

This is very close to our result on the keV scale. When including electron exchange corrections, we find a closer value to this estimate,  $14.5 \text{ keV}$ , but the hundreds of eV difference would be negligible for tunneling in a thermonuclear reaction.

Ionized light nuclei with  $Z = 1$  and plasma thermal energy  $\sim \frac{3}{2}T$  would penetrate the screening cloud of gold up to  $R_{\text{Au}}$  above  $10 \text{ keV}$ . Light nuclei would react in a screened environment at this distance with a considerably reduced internuclear potential  $\sim 14 \text{ keV}$ , enhancing fusion reaction rates as illustrated in Fig. 2.

In principle, one might expect that due to the nonlinear form of Eq. (12), the value of the strong and weak polarization potential would not be additive. However, as discussed in [1] the self-consistent polarization potential at the origin is related to the ultrarelativistic limit of Eq. (15) since  $e\phi(0) \gg m_e$

$$m_{s,\text{FD}}^2(\phi) \approx \frac{4\alpha T^2}{3\pi} \left[ \pi^2 + \frac{\phi^2(r)}{T^2} \right]. \quad (20)$$

Which is simply the weak screening mass plus a strong screening correction. By removing the weakening screening portion, we get a strong screening mass that is independent of temperature

$$m_{s,\text{FD}}(\phi) \approx \sqrt{\frac{4\alpha}{3\pi}} \phi_{\text{vac}}(0), \quad (21)$$

which describes the energy scale of the strong polarization potential at the origin. To get an exact value of the polarization potential at the origin, one could solve the zero temperature limit of Eq. (12) using the ultrarelativistic screening mass

$$-\nabla^2 \phi(r) + \frac{4\alpha}{3\pi} \frac{\phi^3(r)}{(\hbar c)^2} = e\rho_{\text{ext}}(r)/\epsilon_0, \quad (22)$$

which is essentially the ultrarelativistic limit of Thomas-Fermi theory or, in the case of a point charge, the Lane-Emden equation for  $n = 3$ . This additive behavior also implies that calculations of the potential near the origin incorporating nonlinear screening at zero temperature can be added to estimates that calculate the long-distance thermal effects, such as Debye screening, without loss of accuracy. This is likely only the case in plasmas, which are globally weakly coupled, where weak screening is valid at large distances.

The self-consistent strong potential found by solving Eq. (12) is very sensitive to boundary conditions and is only soluble when the form of the potential at large distances is known exactly. We expect that including additional

gold atoms will change the self-consistent strong polarization potential contribution even at large ion separation distances.

#### 4 Enhancement factor for nuclear reaction rates

We will assume that particles participating in reactions will be mostly at the Gamow energy Eq. (3). At this energy, the reacting light nuclei will penetrate up to

$$r_G(E_G) = \frac{Z\alpha\hbar c}{E_G}, \quad (23)$$

which is well into the screening cloud of the gold ion. Furthermore, if the particles are traveling on approximate lines of equipotential energy, they will experience a constant polarization potential over the tunneling integral in the screened cross-section

$$\sigma_{sc}(E) = \frac{S(E)}{E} \exp\left(-\frac{2\sqrt{2\mu}r}{\hbar c} \int_R^{r_c} dr \sqrt{U_{sc}(r_G) - E}\right). \quad (24)$$

The screening enhancement factor, which is the ratio of the reaction rate  $R$  in plasma to vacuum, for thermonuclear reactions with a constant polarization potential is the Salpeter enhancement factor[15]

$$\mathcal{F}_{sc} \equiv \frac{R_{sc}}{R_{vac}} = \exp\left(\frac{U_{vac}(r_G) - U_{sc}(r_G)}{T}\right) = \exp\left(\frac{H(r_G)}{T}\right). \quad (25)$$

The potential  $U_{sc}$  energy between the two nuclei is related to the potential  $\phi$  calculated in Sect. 3 by the self-energy for  $n$  particles

$$U_{sc}(r) = \frac{1}{2} \int d^3r' \rho(r') \phi(r - r') - U(r \rightarrow \infty) = \frac{1}{2} \int d^3r' \left[ \sum_{i \neq j}^n \rho_i(r') \phi_j(r - r') \right]. \quad (26)$$

We consider the self energies of the reacting nuclei and the heavy screening nuclei Where we have subtracted the in-plasma self-energies of the three nuclei separated at  $r \rightarrow \infty$

$$U(r \rightarrow \infty) = \frac{1}{2} \int d^3r' \left[ \sum_{i=j}^n \rho_i(r') \phi_i(r - r') \right]. \quad (27)$$

The total charge density is the sum of the induced plus the external charge density as in Eq. (5). We approximate  $\rho_{ext}$  as a point charge at distances larger than  $R$ , relevant for the tunneling integral and neglect self energies at 2nd order in the polarization charge density  $\rho_{ind}$ . This will give us an underestimated change in the potential energy due to screening

$$U_{sc}(r) = \frac{1}{2} (Z_1 \phi_2 + Z_2 \phi_1) + \frac{Z_3}{2} (\phi_2 + \phi_1) + \frac{Z_1 + Z_2}{2} \phi_3. \quad (28)$$

We choose  $Z_1$  and  $Z_2$  as the charges of the reacting particles and  $Z_3$  as the heavy nucleus. The first term is the usual Salpeter enhancement factor but with a screening mass related to the electron density around the gold nucleus, the second term is the attraction of the gold atom to the polarization clouds of the reacting nuclei, and the final term is the attraction of the reacting nuclei to the polarization cloud of gold.

$$\mathcal{F}_{sc} = \exp\left[\frac{1}{T} \left( Z_1 Z_2 \alpha m_{s,FD}(r_G) + Z_3 \frac{Z_1 + Z_2}{2} \alpha m_{s,FD}(r_G) + \frac{Z_1 + Z_2}{2} \phi_{ind}(r_G) \right)\right]. \quad (29)$$

The screening mass  $m_{s,FD}(r_G)$  is evaluated using the gold potential at  $r_G$ , representing the huge electron density around the gold nucleus. In our calculation, we will assume the turning point is the same for both reacting nuclei, which is only true for  $Z_1 \approx Z_2$ . We will also assume the change in the tunneling probability will be small so that the Gamow energy does not change.

Using these approximations, we arrive at the reaction rate enhancement shown in Fig. 4. The enhancement for each fusion reaction considered p-<sup>11</sup>B, D-T, D-D, and D-<sup>3</sup>He have similar temperature dependence. The slow rise at low temperatures is due to the strong screening contribution that is independent of temperature. The sharp rise above 100 keV is due to the thermal contribution to polarization becoming on the order of the strong screening contribution as seen in Fig. 3. Also, the larger thermal kinetic energy at higher temperatures allows particles to penetrate further into the polarization cloud of gold. The enhancement flattens out at temperatures greater than the electron mass  $m_e$  since there the electron polarization cloud is well described by the Debye screening mass Fig. 11, which scales linearly with temperature in the ultrarelativistic limit, giving a constant enhancement factor.

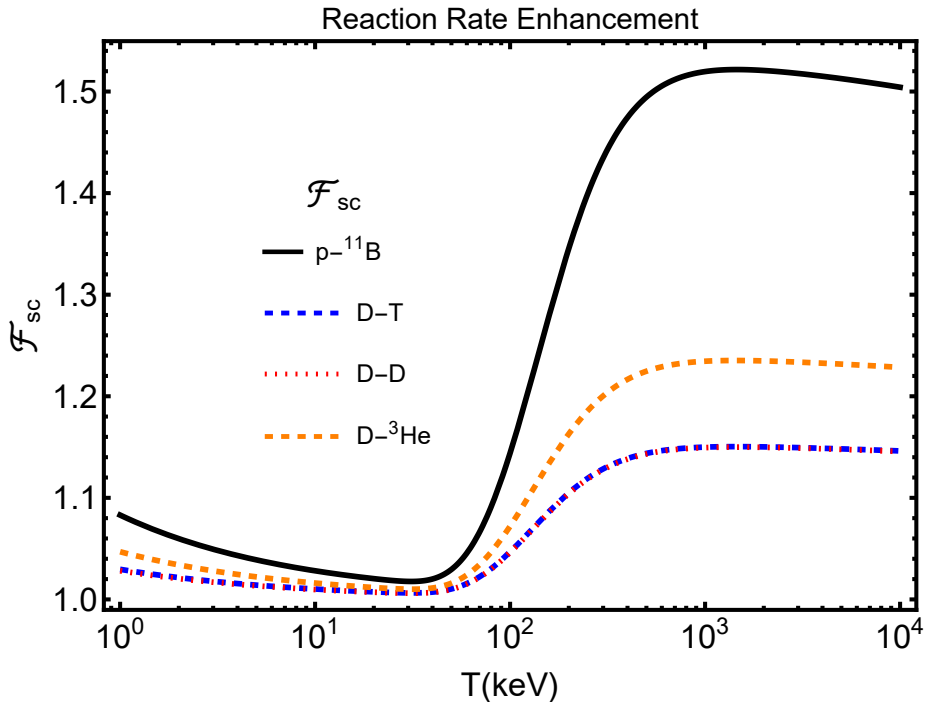


**Fig. 4.** Reaction rate enhancement  $\mathcal{F}_{sc}$  [see Eq. (29)] for various fusion reactions as a function of temperature in keV: p- $^{11}\text{B}$  as a black solid line, D-T as a dashed blue line, D-D as a dotted red line, and D- $^3\text{He}$  as a dashed orange line.

Looking at each individual reaction, we can see that the largest effect on the enhancement is due to the size of  $Z_1$  and  $Z_2$ . This is because a larger  $Z$  more strongly attracts the local electron density to screen the reacting nuclei. This leads to p- $^{11}\text{B}$  having the largest enhancement factor since boron has  $Z_2 = 5$ . The enhancement for each nuclear reaction is considerable and should be measurable in an experiment. Weak screening predicts much smaller changes to nuclear reaction rates [36,37].

## 5 Conclusion and discussion

This work introduces the concept that fusion reactions may proceed more easily in the presence of “heavy nuclear catalysts” using a simple model of a heavy nucleus in an equilibrium plasma. Heavy catalysts are nuclei with a high atomic number ( $Z$ ) that provide a ‘condensation’ domain with a dense screening cloud of electrons. This environment allows higher energy light nuclei to undergo thermonuclear reactions with a significantly reduced Coulomb barrier by the high electron density.

We implemented self-consistent strong electron plasma screening near such a high atomic number nucleus to determine the short-range polarization potential relevant to thermonuclear reactions in an electron-ion plasma. We have in mind applications that arise, for example, when fusible material is found near such catalysts in the initial phases of laser interaction with gold nanorod-doped targets [7,8,9,10,11,12].

We address the behavior of electron plasma at keV energies, which can be created through laser-matter interactions with intensities of  $10^{17} - 10^{20}$  W/cm $^2$  over timescales of roughly 20 femtoseconds. During this brief period, electrons in the plasma can achieve approximate thermal equilibrium. In contrast, the heavier ions remain immobile and do not contribute to the screening process other than by creating a location where many electrons coalesce. Using this picture, we use the equilibrium approach to solve the Poisson-Fermi-Dirac equation developed in [1]. A more complete plasma dynamics in self-consistent strong screening will be explored in future studies. The objective of this article is not to provide a definitive estimate of the enhancement of fusion reactions plasma but to improve on past works and to indicate that the effect of heavy nuclear catalysts could be measurable in experiments.

We comment on works by [38,39] study similar strong screening enhancement in plasmas where an ion beam interacts with a cold electron gas, providing an electron density higher than the equilibrium density used here. We note that [38,39] calculate much larger enhancements of thermonuclear reaction rates since they use a Boltzmann distribution for the electron density.

In Fig. 3, we determined the polarization potential  $e\phi_{ind}$  for gold nuclei in an equilibrium electron-ion plasma at various temperatures. We find that fusion reactions of light nuclei occurring in the large electron cloud around a gold nucleus ( $Z = 79$ ) experience a keV scale lowering of the Coulomb barrier.

The enhancement for p- $^{11}\text{B}$  fusion is largest at temperatures above 100 keV. At these temperatures, both the semi-bound and plasma screening electrons contribute. This effect is large enough, a factor  $\sim 1.5$  enhancement,

to be measured in future experiments of fusion reaction rates in plasma [5] and could be relevant for fusion in laser-generated fusion plasmas. This enhancement is most likely underestimated since we neglected contributions to the self-energy above linear order in the polarization charge Eq. (28), which may not be small. Moreover, enhancement is also predicted at low temperatures due to the bound gold electrons. The enhancement calculated here assumes reacting nuclei can only penetrate the electron cloud due to their thermal energy. If the reacting ions were non-thermal, for example, when generated by a (laser-accelerated) particle beam, they would penetrate much further into the electron cloud, yielding an enhancement rate on the order of

$$\mathcal{F}_{\text{sc}} = \exp\left(\frac{\langle Z \rangle e \phi_{\text{ind}}(R)}{T}\right), \quad (30)$$

where  $\langle Z \rangle$  is the average atomic number of the reactants and  $e \phi_{\text{ind}}(R) \approx 14 \text{ keV}$ . This would lead to even larger enhancement and could be relevant for measuring nuclear cross-section in metallic environments [40].

Historically, experimental determinations of astrophysical S-factors have found anomalous screening at low temperatures [41, 42, 43, 44]. This anomalous screening was measured recently [45] again. The experimental results were never fully consistent regarding the screening magnitude, suggesting that some environmental properties were not fully controlled. In view of our results, we speculate the presence of target contamination by a catalyst, which at low temperatures achieved by intense beams could help explain anomalous screening at low collision energy.

The enhancement from heavy nuclear catalysts increases with the average atomic number  $\langle Z \rangle > 2$  of the fusing nuclei, indicating catalysis is more beneficial for medium- $Z$  reactions,  $\langle Z \rangle > 2$ , such as p- $^{11}\text{B}$ . This is because such reacting nuclei more strongly attract local electron density, allowing stronger screening. The enhancement also increases with increasing catalyst atomic number  $Z$  due to the increase in density of the electron screening cloud.

Another interesting finding of this work is that the contribution to polarization potential at the origin from self-consistent strong screening is independent of temperature. This separation offers major simplifications to the determination screening enhancement of thermonuclear reactions. The self-consistent strong screening contribution to the potential can be estimated at zero temperature  $e \phi / T \gg 1$  using the Thomas-Fermi model Eq. (22) or some equivalent model of the electron density around an atom. Then, thermal effects at large distances can be considered separately and summed up in the final result. In future studies, we will determine if this separation of thermal and strong screening also applies to a dynamic plasma.

In future theoretical work, we plan to improve our understanding of nuclear catalysts by addressing the limitations of our current model. A key simplifying assumption made to make our model soluble was equilibrium for electrons in the plasma. This is generally never true in laser-generated plasmas, which display mostly nonequilibrium behavior. A semi-analytical description of nonequilibrium effects through linear response may be possible in a combined dynamic-strong plasma theory. Additionally, while gold was treated as fully ionized in this study due to the high-temperature plasma context, in future calculations, we would like to describe the low-temperature quantum environment of the solid fusion target where conducting electrons contribute to the screening effect in a coherent response to the external field.

We foresee an opportunity for experimental work in the near future dedicated to studying nuclear reactions in the presence of catalysts. This will help understand some ongoing screening enhancement riddles relevant to BBN and element genesis in stellar explosions. We can imagine a rather simple experimental setup for studying heavy catalysis of fusion reactions: An inverse kinematic experiment in which a heavy metal proton-hydride is the target for the Boron beam. Also, a slightly more sophisticated setup with a colliding beam p-11B interaction point that lies within a thin gold foil. Such an experimental program is long overdue, seen the long-term riddle of screening effects in low-energy nuclear reactions.

### Acknowledgement:

We thank Tamas Biró and the Wigner Hun-REN Research Center for their kind hospitality in Budapest during the PP2024 conference, supported by NKFIH (Hungarian National Office for Research, Development and Innovation) under awards 2022-2.1.1-NL-2022-00002 and 2020-2.1.1-ED-2024-00314. This meeting and the related research report motivate the presentation of these recently obtained results.

CG gratefully acknowledges financial support for this research by the Fulbright U.S. Scholar Program, sponsored by the U.S. Department of State, the Hungarian Fulbright Commission, and the Hungarian Academy of Sciences under award FBM2024-2. Its contents are solely the author's responsibility and do not necessarily represent the official views of the Fulbright Program, the Government of the United States, or the Hungarian Fulbright Commission. JR did not receive sponsor funding for this work.

### Data Availability Statement:

No datasets were generated or analyzed during the current study.

### References

1. C. Grayson, C.T. Yang, M. Formanek, J. Rafelski, Self-consistent strong screening applied to thermonuclear reactions. *The Astrophysical Journal* **976**(1), 31 (2024). doi:[10.3847/1538-4357/ad7dee](https://doi.org/10.3847/1538-4357/ad7dee). URL <https://dx.doi.org/10.3847/1538-4357/ad7dee>



2. E. Fourkal, I. Velchev, C.M. Ma, Coulomb explosion effect and the maximum energy of protons accelerated by high-power lasers. *Phys. Rev. E* **71**, 036412 (2005). doi:[10.1103/PhysRevE.71.036412](https://doi.org/10.1103/PhysRevE.71.036412). URL <https://link.aps.org/doi/10.1103/PhysRevE.71.036412>
3. J. Braenzel, A.A. Andreev, K. Platonov, M. Klingsporn, L. Ehrentraut, W. Sandner, M. Schnürer, Coulomb-driven energy boost of heavy ions for laser-plasma acceleration. *Phys. Rev. Lett.* **114**, 124801 (2015). doi:[10.1103/PhysRevLett.114.124801](https://doi.org/10.1103/PhysRevLett.114.124801). URL <https://link.aps.org/doi/10.1103/PhysRevLett.114.124801>
4. O. Hurricane, D. Callahan, D. Casey, P. Celliers, C. Cerjan, E. Dewald, T. Dittrich, T. Döppner, D. Hinkel, L.B. Hopkins, et al., Fuel gain exceeding unity in an inertially confined fusion implosion. *Nature* **506**(7488), 343–348 (2014)
5. D.T. Casey, C.R. Weber, A.B. Zylstra, C.J. Cerjan, E. Hartouni, M. Hohenberger, L. Divol, D.S. Dearborn, N. Kabadi, B. Lahmann, et al., Towards the first plasma-electron screening experiment. *Frontiers in Physics* **10**, 1057603 (2023)
6. S. Vallières, M. Salvadori, A. Permogorov, G. Cantono, K. Svendsen, Z. Chen, S. Sun, F. Consoli, E. d’Humières, C.G. Wahlström, et al., Enhanced laser-driven proton acceleration using nanowire targets. *Scientific Reports* **11**(1), 2226 (2021)
7. I. Papp, L. Bravina, M. Csete, A. Kumari, I.N. Mishustin, D. Molnár, A. Motornenko, P. Rácz, L.M. Satarov, H. Stöcker, D.D. Strottmann, A. Szenes, D. Vass, T.S. Biró, L.P. Csernai, N. Kroó, Kinetic model evaluation of the resilience of plasmonic nanoantennas for laser-induced fusion. *PRX Energy* **1**, 023001 (2022). doi:[10.1103/PRXEnergy.1.023001](https://doi.org/10.1103/PRXEnergy.1.023001). URL <https://link.aps.org/doi/10.1103/PRXEnergy.1.023001>
8. T.S. Biró, N. Kroó, L.P. Csernai, M. Veres, M. Aladi, I. Papp, M.A. Kedves, J. Kámán, A. Nagyné Szokol, R. Holomb, I. Rigó, A. Bonyár, A. Borók, S. Zangana, R. Kovács, N. Tarpataki, M. Csete, A. Szenes, D. Vass, E. Tóth, G. Galbács, M. Szalóki, With nanoplasmonics towards fusion. *Universe* **9**(5) (2023). doi:[10.3390/universe9050233](https://doi.org/10.3390/universe9050233). URL <https://www.mdpi.com/2218-1997/9/5/233>
9. L.P. Csernai, I.N. Mishustin, L.M. Satarov, H. Stöcker, L. Bravina, M. Csete, J. Kámán, A. Kumari, A. Motornenko, I. Papp, et al., Crater formation and deuterium production in laser irradiation of polymers with implanted nanoantennas. *Physical Review E* **108**(2), 025205 (2023)
10. L. Csernai, T. Csörgő, I. Papp, K. Tamosiunas, M. Csete, A. Szenes, D. Vass, T. Biró, N. Kroó, Femtoscopy for the nano-plasmonic laser inertial fusion experiments (naplife) project. *Universe* **10**(4), 161 (2024)
11. Ágnes Nagyné Szokol, J. Kámán, R. Holomb, M. Aladi, M. Kedves, B. Ráczkevi, P. Rácz, A. Bonyár, A. Borók, S. Zangana, M. Szalóki, I. Papp, G. Galbács, T.S. Biró, L.P. Csernai, N. Kroó, M. Veres, N. Collaboration. Pulsed laser intensity dependence of crater formation and light reflection in the udma-tegdma copolymer nanocomposite, doped with resonant plasmonic gold nanorods (2024). URL <https://arxiv.org/abs/2402.18138>
12. I. Papp, L. Bravina, M. Csete, A. Kumari, I.N. Mishustin, A. Motornenko, P. Rácz, L.M. Satarov, H. Stöcker, A. Szenes, D. Vass, T.S. Biró, L.P. Csernai, N. Kroó. Pic simulations of laser-induced proton acceleration by resonant nanoantennas for fusion (2024). URL <https://arxiv.org/abs/2306.13445>
13. N. Kroó, L. Csernai, I. Papp, M. Kedves, M. Aladi, A. Bonyár, M. Szalóki, K. Osvay, P. Varmazyar, T. Biró, Indication of p+ 11b reaction in laser induced nanofusion experiment. *Scientific Reports* **14**(1), 1–8 (2024)
14. L.P. Csernai, T. Csörgő, I. Papp, K. Tamosiunas, M. Csete, A. Szenes, D. Vass, T.S. Biró, N. Kroó, Radiation pattern and source size of particles in nanoplasmonic fusion (2023). [arXiv:2309.05156](https://arxiv.org/abs/2309.05156) [physics.plasm-ph]
15. E.E. Salpeter, Electron screening and thermonuclear reactions. *Austral. J. Phys.* **7**, 373–388 (1954). doi:[10.1071/PH540373](https://doi.org/10.1071/PH540373)
16. P. Debye, E. Hückel, Zur theorie der elektrolyte. *Physikalische Zeitschrift* **24**, 185–206 (1923)
17. N.J. Shaviv, G. Shaviv, The electrostatic screening of thermonuclear reactions in astrophysical plasmas. i. *Astrophys. J.* **468**, 433 (1996). doi:[10.1086/177702](https://doi.org/10.1086/177702)
18. H. Dzitko, S. Turck-Chieze, P. Delbourgo-Salvador, C. Lagrange, The screened nuclear reaction rates and the solar neutrino puzzle. *Astrophysical Journal* **447**, 428 (1995). doi:[10.1086/175887](https://doi.org/10.1086/175887)
19. A.V. Gruzinov, J.N. Bahcall, Screening in thermonuclear reaction rates in the sun. *Astrophys. J.* **504**, 996–1001 (1998). doi:[10.1086/306116](https://doi.org/10.1086/306116). [arXiv:astro-ph/9801028](https://arxiv.org/abs/astro-ph/9801028) [astro-ph]
20. M. Brüggén, D.O. Gough, On electrostatic screening of ions in astrophysical plasmas. *Astrophys. J.* **488**(2), 867–871 (1997). doi:[10.1086/304718](https://doi.org/10.1086/304718). [arXiv:astro-ph/9702102](https://arxiv.org/abs/astro-ph/9702102) [astro-ph]
21. M. Brüggén, D.O. Gough, Free energy of a screened ion pair. *Journal of Mathematical Physics* **41**, 260–283 (2000)
22. S.L. Bi, M.P.D. Mauro, J. Christensen-Dalsgaard, Coulomb corrections to the equation of state for a weakly-coupled plasma. *Astron. Astrophys.* **364**, 157–164 (2000)
23. T.E. Liolios, Weakly screened thermonuclear reactions in astrophysical plasmas: Improving salpeter’s model. *Eur. Phys. J. A* **18**, s1–s25 (2004). doi:[10.1140/epjad/s2003-01-001-7](https://doi.org/10.1140/epjad/s2003-01-001-7)
24. Y. Luo, M.A. Famiano, T. Kajino, M. Kusakabe, A.B. Balantekin, Screening corrections to electron capture rates and resulting constraints on primordial magnetic fields. *Phys. Rev. D* **101**(8), 083010 (2020). doi:[10.1103/PhysRevD.101.083010](https://doi.org/10.1103/PhysRevD.101.083010)
25. P. Mora, Plasma expansion into a vacuum. *Phys. Rev. Lett.* **90**, 185002 (2003). doi:[10.1103/PhysRevLett.90.185002](https://doi.org/10.1103/PhysRevLett.90.185002). URL <https://link.aps.org/doi/10.1103/PhysRevLett.90.185002>
26. S. Bochkarev, V.Y. Bychenkov, V. Tikhonchuk, Investigation of ion acceleration in an expanding laser plasma by using a hybrid boltzmann-vlasov-poisson model. *Plasma physics reports* **32**, 205–221 (2006)
27. H.E. Dewitt, H.C. Graboske, M.S. Cooper, Screening factors for nuclear reactions. i. general theory. *Astrophysical Journal* **181**, 439–456 (1973)
28. N. Itoh, H. Totsuji, S. Ichimaru, Enhancement of thermonuclear reaction rate due to strong screening. *Astrophysical Journal* **218**, 477 (1977). doi:[10.1086/155701](https://doi.org/10.1086/155701)
29. N. Itoh, H. Totsuji, S. Ichimaru, H.E. DeWitt, Enhancement of thermonuclear reaction rate due to strong screening. ii - ionic mixtures. *Astrophysical Journal* **234**, 1079 (1979). doi:[10.1086/157590](https://doi.org/10.1086/157590)

30. S. Ichimaru, Strongly coupled plasmas: high-density classical plasmas and degenerate electron liquids. *Rev. Mod. Phys.* **54**(4), 1017–1059 (1982). doi:[10.1103/RevModPhys.54.1017](https://doi.org/10.1103/RevModPhys.54.1017)
31. A.I. Chugunov, H.E. DeWitt, D.G. Yakovlev, Coulomb tunneling for fusion reactions in dense matter: Path integral Monte Carlo versus mean field. *Phys. Rev. D* **76**, 025028 (2007). doi:[10.1103/PhysRevD.76.025028](https://doi.org/10.1103/PhysRevD.76.025028). arXiv:[0707.3500](https://arxiv.org/abs/0707.3500) [astro-ph]
32. A.I. Chugunov, H.E. DeWitt, Nuclear fusion reaction rates for strongly coupled ionic mixtures. *Phys. Rev. C* **80**, 014611 (2009). doi:[10.1103/PhysRevC.80.014611](https://doi.org/10.1103/PhysRevC.80.014611). arXiv:[0905.3844](https://arxiv.org/abs/0905.3844) [astro-ph.SR]
33. P.A. Kravchuk, D.G. Yakovlev, Strong plasma screening in thermonuclear reactions: Electron drop model. *Phys. Rev. C* **89**(1), 015802 (2014). doi:[10.1103/PhysRevC.89.015802](https://doi.org/10.1103/PhysRevC.89.015802). arXiv:[1401.2539](https://arxiv.org/abs/1401.2539) [astro-ph.SR]
34. H. De Vries, C. De Jager, C. De Vries, Nuclear charge-density-distribution parameters from elastic electron scattering. *Atomic Data and Nuclear Data Tables* **36**(3), 495–536 (1987). doi:[https://doi.org/10.1016/0092-640X\(87\)90013-1](https://doi.org/10.1016/0092-640X(87)90013-1). URL <https://www.sciencedirect.com/science/article/pii/0092640X87900131>
35. W.R. Garrett, C.P. Bhalla, Potential energy shift for a screened coulomb potential. *Zeitschrift für Physik* **198**, 453–460 (1967). URL <https://api.semanticscholar.org/CorpusID:119972363>
36. E. Hwang, D. Jang, K. Park, M. Kusakabe, T. Kajino, A.B. Balantekin, T. Maruyama, C.M. Ryu, M.K. Cheoun, Dynamical screening effects on big-bang nucleosynthesis. *JCAP* **11**, 017 (2021). doi:[10.1088/1475-7516/2021/11/017](https://doi.org/10.1088/1475-7516/2021/11/017). arXiv:[2102.09801](https://arxiv.org/abs/2102.09801) [nucl-th]
37. C. Grayson, C.T. Yang, M. Formanek, J. Rafelski, Electron–positron plasma in bbn: Damped-dynamic screening. *Annals Phys.* **458**, 169453 (2023). doi:[10.1016/j.aop.2023.169453](https://doi.org/10.1016/j.aop.2023.169453). arXiv:[2307.11264](https://arxiv.org/abs/2307.11264) [astro-ph.CO]
38. Y. Wu, A. Pálffy, Determination of plasma screening effects for thermonuclear reactions in laser-generated plasmas. *Astrophys. J.* **838**(1), 55 (2017). doi:[10.3847/1538-4357/aa6252](https://doi.org/10.3847/1538-4357/aa6252). arXiv:[1612.06884](https://arxiv.org/abs/1612.06884) [physics.plasm-ph]
39. D. Elsing, A. Pálffy, Y. Wu, Quantum effects on plasma screening for thermonuclear reactions in laser-generated plasmas. *Phys. Rev. Res.* **4**(2), L022004 (2022). doi:[10.1103/PhysRevResearch.4.L022004](https://doi.org/10.1103/PhysRevResearch.4.L022004)
40. A. Huke, K. Czerski, P. Heide, G. Ruprecht, N. Targosz, W. Żebrowski, Enhancement of deuteron-fusion reactions in metals and experimental implications. *Phys. Rev. C* **78**, 015803 (2008). doi:[10.1103/PhysRevC.78.015803](https://doi.org/10.1103/PhysRevC.78.015803). URL <https://link.aps.org/doi/10.1103/PhysRevC.78.015803>
41. U. Schröder, S. Engstler, A. Krauss, K. Neldner, C. Rolfs, E. Somorjai, K. Langanke, Search for electron screening of nuclear reactions at sub-coulomb energies. *Nuclear Instruments and Methods in Physics Research Section B: Beam Interactions with Materials and Atoms* **40-41**, 466–469 (1989). doi:[https://doi.org/10.1016/0168-583X\(89\)91022-7](https://doi.org/10.1016/0168-583X(89)91022-7). URL <https://www.sciencedirect.com/science/article/pii/0168583X89910227>
42. T.D. Shoppa, S.E. Koonin, K. Langanke, R. Seki, One- and two-electron atomic screening in fusion reactions. *Phys. Rev. C* **48**, 837–840 (1993). doi:[10.1103/PhysRevC.48.837](https://doi.org/10.1103/PhysRevC.48.837). URL <https://link.aps.org/doi/10.1103/PhysRevC.48.837>
43. M. Aliotta, F. Raiola, G. Gyürky, A. Formicola, R. Bonetti, C. Brogini, L. Campajola, P. Corvisiero, H. Costantini, A. D’Onofrio, Z. Fülöp, G. Gervino, L. Gialanella, A. Guglielmetti, C. Gustavino, G. Imbriani, M. Junker, P. Moroni, A. Ordine, P. Prati, V. Roca, D. Rogalla, C. Rolfs, M. Romano, F. Schümann, E. Somorjai, O. Straniero, F. Strieder, F. Terrasi, H. Trautvetter, S. Zavatarelli, Electron screening effect in the reactions  $3\text{He}(d,p)4\text{He}$  and  $d(3\text{He},p)4\text{He}$ . *Nuclear Physics A* **690**(4), 790–800 (2001). doi:[https://doi.org/10.1016/S0375-9474\(01\)00366-9](https://doi.org/10.1016/S0375-9474(01)00366-9). URL <https://www.sciencedirect.com/science/article/pii/S0375947401003669>
44. K. Czerski, A. Huke, A. Biller, P. Heide, M. Hoefft, G. Ruprecht, Enhancement of the electron screening effect for  $d + d$  fusion reactions in metallic environments. *Europhysics Letters* **54**(4), 449 (2001). doi:[10.1209/epl/i2001-00265-7](https://doi.org/10.1209/epl/i2001-00265-7). URL <https://dx.doi.org/10.1209/epl/i2001-00265-7>
45. Q. Zhang, Z. Huang, J. Hu, B. Chen, S. Hou, T. Wang, K. Fang, Astrophysical S(E) for the  ${}^9\text{Be}(p, d){}^8\text{Be}$  and  ${}^9\text{Be}(p, \alpha){}^6\text{Li}$  Reactions by Direct Measurement. *APJ* **893**(2), 126 (2020). doi:[10.3847/1538-4357/ab8222](https://doi.org/10.3847/1538-4357/ab8222)